An x-ray diffraction and EXAFS study of the electric-field-induced $PbZrO_3$ ferroelectric phase

1996 J. Phys.: Condens. Matter 8 1615

(http://iopscience.iop.org/0953-8984/8/11/007)

J. Phys.: Condens. Matter **8** (1996) 1615–1620. Printed in the UK

An x-ray diffraction and EXAFS study of the electric-field-induced $PbZrO_3$ ferroelectric phase

V A Shuvaeva†, M Yu Antipin‡, O E Fesenko† and Yu T Struchkov†§

† Institute of Physics, Rostov State University, Stachky Street 194, Rostov-on-Don, 344104, Russia

‡ Institute of Organoelement Compounds, Russian Academy of Sciences, Vavilov Street 28, Moscow B-334, Russia

Received 7 June 1995, in final form 2 November 1995

Abstract. A structural study of a $PbZrO_3$ electric-field-induced ferroelectric phase has been performed using single-crystal x-ray diffraction and EXAFS techniques. The polar axis was found to be orthogonal to the direction of atomic displacements in the initial antiferroelectric phase. The ferroelectric properties of the phase are due to a Pb displacement of about 0.17 Å relative to the oxygen framework along the polar axis. The Zr atoms are disordered between two symmetry-related positions and shifted mainly orthogonally to the polar axis. The results obtained by the two methods of crystal structure investigation are in good agreement.

1. Introduction

$PbZrO_3$ is a classic antiferroelectric, as a ferroelectric phase may be induced in this crystal by applying an electric field. Optical study of the electric-field-induced (EFI) phase transitions in the temperature interval from 100 to 500 K [1] revealed three ferroelectric phases in this material: two of them are rhombohedral and one orthorhombic. The rhombohedral phases were supposed to be similar to the ferroelectric phases of $PbTi_xZr_{1-x}O_3$ solid solutions [2]. The orthorhombic phase has not been found in $PbZrO_3$ and its solid solutions without any electric field applied. It was supposed that this phase was similar to the orthorhombic phase of $KNbO_3$ [3]. Later the space group of this phase was found to be $Cm2m$ [4]. Here we report the results of x-ray diffraction and EXAFS structural studies of this phase.

2. Experimental procedure

For the experiments very thin (about 20 μm thick) plate-like single crystals were selected. Almost all of the surfaces of the crystal major faces orthogonal to the [100] perovskite direction were covered with conducting graphite layers for applying the electric field. For the crystal being investigated by x-ray diffraction the absence of twinning in the initial phase and the EFI phase (which arose at $\simeq$220 kV cm^{-1}) was ascertained by observation in polarized light (crossed Nicols), and by examination of the shape of the x-ray reflection profile and comparison of equivalent-reflection intensities. As a result of the phase transition, the intensities of the reflections with $k = 2n$, $l = 2n$ of the initial antiferroelectric phase were observed to become not more than 3σ, so the a- and b-parameters are approximately two

§ Deceased.

0953-8984/96/111615+06$19.50

times smaller than those of the initial phase [5]. A constant electric field of 250 kV cm^{-1} was maintained for the single-crystal samples during the experiments.

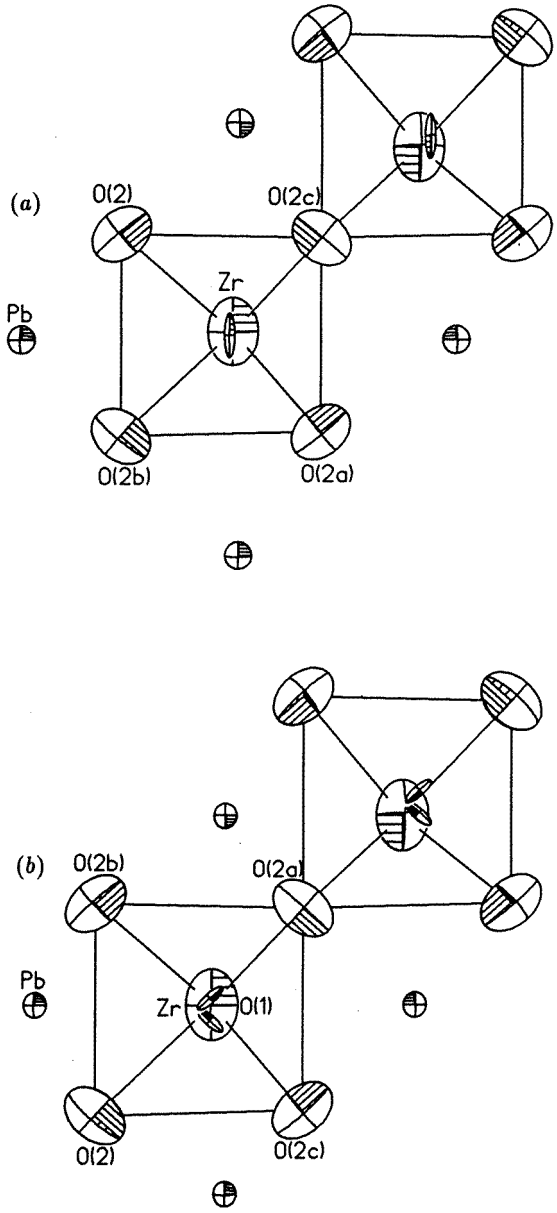

Figure 1. A projection of the $PbZrO_3$ EFI phase structure on the (001) plane. Upper panel: Zr in the *m*2*m* position. Lower panel: Zr disordered among two symmetry-related positions.

X-ray diffraction data were collected with a Siemens P3/PC diffractometer (Mo Kα radiation, graphite monochromator, $\theta/2\theta$-scan, 480 independent observable reflections). At room temperature, the cell parameters were found to be: $a = 5.890(1)$, $b = 5.897(1)$, $c = 4.134(1)$ Å, $V = 143.59(7)$ $Å^3$, $\mu = 62.35$ mm^{-1}. These are in agreement with results

reported in [4].

The Zr K-edge EXAFS spectra were obtained in the transmission mode below and above the EFI phase transition point. The experiment was performed using the laboratory spectrometer with a bent-Si(1230)-crystal monochromator [6] equipped with an Mo-anode x-ray tube and an NaI scintillation detector. The voltage and anode current were equal to 28 kV and 28 mA respectively. The energy resolution was estimated from the Zr-edge width to be not more than 11 eV. The spectra were measured at 330 points in the energy range from 18 700 to 19 800 eV.

Table 1. Atomic coordinates (multiplied by 10^4) and temperature factors (in units of 10^3 Å^2) in the $PbZrO_3$ EFI phase.

Atom	x	y	z	U_{iso}		
Pb	0	0	0	12(1)		
Zr, model 1	0	4679(6)	5000	23(1)		
Zr, model 2	279(5)	4700(7)	5000	18(1)		
O(1)	0	4264(36)	0	107(2)		
O(2)	2831(30)	2356(27)	5000	83(2)		
Atom	U_{11}	U_{22}	U_{33}	U_{23}	U_{13}	U_{12}
Pb	13(1)	11(1)	12(1)	0	0	0
Zr, model 1	47(2)	3(2)	18(1)	0	0	0
Zr, model 2	14(1)	18(2)	20(1)	0	0	15(1)
O(1)	137(4)	73(4)	111(4)	0	0	0
O(2)	75(4)	54(4)	119(4)	0	0	59(6)

3. Data reduction

Our x-ray diffraction study supported the conclusion reached previously [4], that the space group of the $PbZrO_3$ EFI phase is $Cm2m$ (here we retain the correspondence of axes of the initial and EFI phases). Refinement of the structure with Zr atoms in the special $m2m$ symmetry position led to a highly irregular shape of the Zr thermal ellipsoid and very high values of its temperature displacement amplitudes orthogonal to the polar axis. We supposed that this was an effect of the Zr position disorder. Refinement of the structural model in the same space group but with the Zr atoms equally distributed between two symmetry-related positions in the (100) plane reduced the R-value relative to that for the completely ordered model from 8.9% to 6.8%. Refinement results are presented in table 1. Projections of the structures on the (001) plane for both models are shown in figure 1. As may be seen, thermal ellipsoids of Zr atoms remained quite anisotropic in the second model also, although mean square displacement amplitudes became smaller. Attempts at obtaining further detail on Zr positions led to a strong correlation being found between its positional and thermal parameters. Refinement on the basis of 480 high-angle reflections yielded $R = 4.8\%$ and more reliable oxygen position parameters. Zr–O interatomic distances for the initial antiferroelectric phase previously obtained in [5] and those calculated for both models of the EFI phase are presented in table 2.

The EXAFS data were analysed by well-established procedures (background removal using a Victoreen function for pre-edge extrapolation, the location of E_0 set at the edge at the point of inflection of $\mu(E)$). The Fourier transform (FT) EXAFS study of the $k^3\chi(k)$-data was performed over a k-range from 3 to 13.5 Å^{-1} without correction for phase shifts.

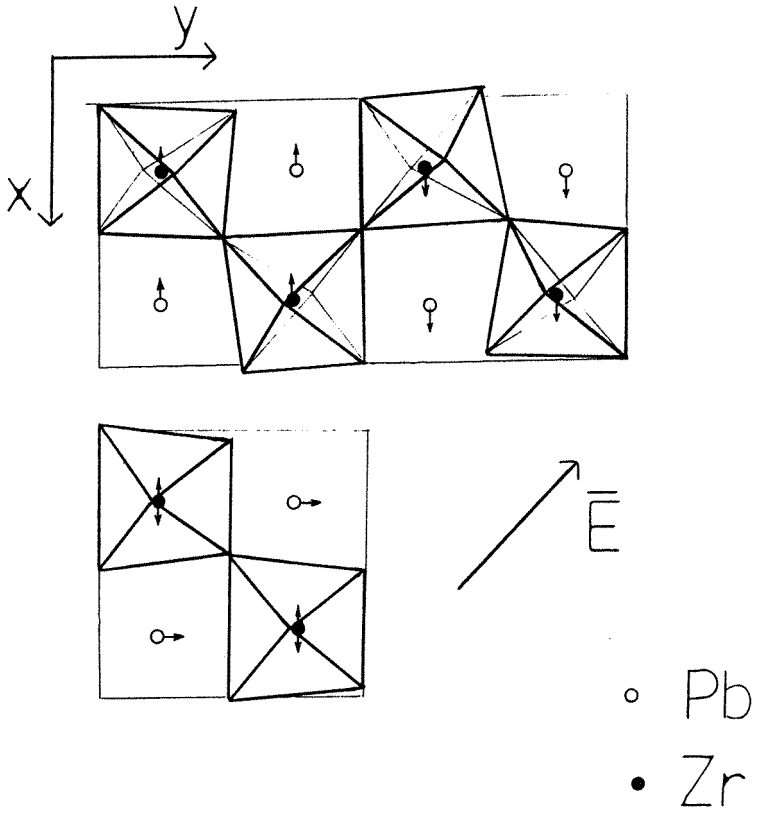

Figure 2. The direction of cation displacement in the antiferroelectric (upper panel) and EFI (lower panel) phases of $PbZrO_3$.

Table 2. The interatomic Zr–O distances (Å) in the initial antiferroelectric and EFI phases.

Antiferroelectric phase	EFI phase (model 1)	EFI phase (model 2)
2.01	2.07(1)	1.92(1)
2.06	2.07(1)	2.04(1)
2.10	2.08(3)	2.09(3)
2.10	2.08(3)	2.09(3)
2.13	2.10(3)	2.13(3)
2.21	2.10(3)	2.30(3)

4. Results and discussion

The ferroelectric properties of the $PbZrO_3$ EFI phase are due to ferroelectric ordering of Pb displacements relative to the oxygen framework along the polar axis. The space group $Cm2m$ adopted for the EFI phase indicates that the polar axis direction is orthogonal to the direction of antiferroelectric atomic displacements in the initial phase. The directions of Zr atomic shifts from the oxygen octahedra centres are close to those in the initial phase and orthogonal to the polar axis. However, these shifts are probably not ordered in the EFI phase, as superstructural reflections which were due to antiferroelectric ordering of atomic

displacements in the initial phase vanish during the EFI phase transition. So, the electric field does not polarize the Zr sublattice but only destroys the ordering of Zr antiferroelectric displacements. The directions of atomic shifts in both phases in the (100) plane are shown in figure 2. The oxygen octahedra in the EFI phase are untilted. Their distortion is close to that in the initial phase.

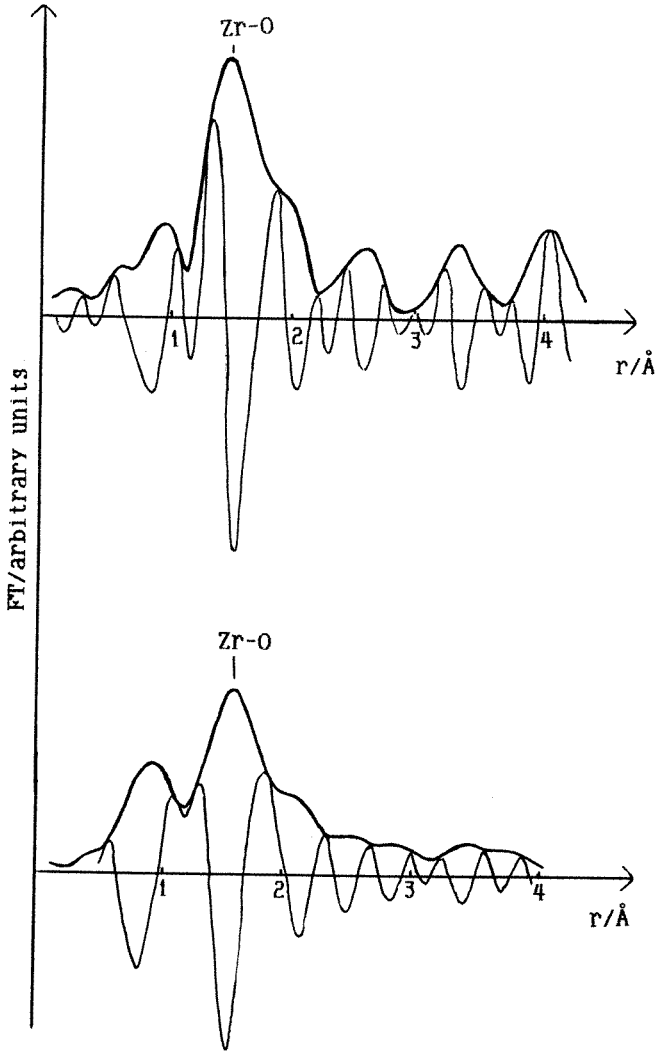

Figure 3. The magnitudes and imaginary parts of the Fourier transforms of k^3-weighted EXAFS for $PbZrO_3$. Upper panel: the initial antiferroelectric phase. Lower panel: the EFI phase.

As to thermal parameters, they seem to be too large for all atoms. However, Pb mean square displacements correspond to those reported for the antiferroelectric phase [5]. It should be noted that Pb thermal vibrations are quite isotropic. Very high values of Zr thermal parameters are possibly due to more complicated distribution of the atoms within octahedra than was assumed in the refined models. Oxygen anisotropic temperature parameter determination is not really accurate enough, but it may suggest that high oxygen

thermal parameter values are due to instability of the structure with respect to octahedra tilting. The high values of oxygen mean square displacements in the planes orthogonal to Zr–O bonds which were obtained in the high-order refinement, as well as the too extreme values of the smallest and the largest Zr–O distances obtained for model 2, also support this suggestion.

It has been shown that the EXAFS technique in some cases permits one to resolve atomic positions in perovskite-type compounds [7–9]. In the case of $PbZrO_3$ as can be seen from table 2, the oxygen shell around the Zr atom is spilt into several close subshells. Due to the great number of parameters the conventional fitting procedure is not appropriate in this case. However, radial atomic distributions in the two models of the EFI phase are quite different. In model 1 deviations of Zr–O distances from their average value are much smaller than in the initial phase, while model 2 assumes the growth of disorder in the oxygen shell. Hence, it is even possible to verify additionally the validity of the structural models of the EFI phase through qualitative analysis of EXAFS.

The FT EXAFS of the $PbZrO_3$ initial antiferroelectric phase shown in figure 3, upper panel, exhibits two oxygen peaks at about $r = 1.9$ Å originating from the splitting of the first shell into several close subshells. In the EFI phase (figure 3, lower panel) the Zr–O peak is not split but its amplitude is smaller than that in the initial phase. Such behaviour indicates the growth of disorder in the oxygen shell. Hence the local structure evolution can be explained only when taking account of the Zr disorder, as in model 2 for the EFI phase. More accurate EXAFS studies of the EFI phase transition are in progress.

Thus, the EFI phase transition in $PbZrO_3$ significantly differs from that in $NaNbO_3$ where applying an electric field results simply in reversal of the atomic shift direction in half of the initial cell [10]. The $Cm2m$ $PbZrO_3$ phase is intermediate between the antiferroelectric phase and the $R3m$ ferroelectric phase arising in stronger electric fields which is expected to have a completely ordered ferroelectric structure.

Acknowledgments

This work was supported by the International Science Foundation (Grant M1F300) and the Russian Fundamental Investigations Foundation (project N 95-02-05716A). This support is gratefully acknowledged.

References

[1] Fesenko O E and Smotrakov V G 1976 *Ferroelectrics* **12** 211–3
[2] Michel C, Moreau J M and Achenbach J D 1969 *Solid State Commun.* **7** 865–72
[3] Fesenko O E, Kolesova R V and Sindeev Yu G 1979 *Fiz. Tverd. Tela* **21** 1152–9
[4] Kolesova R V, Leontiev N G, Smotrakov V G and Fesenko O E 1981 *VINITI Report* 3760–81 (deposited 24.07.81)
[5] Fujishita H, Shiozaki Yo, Achiwa N and Sawaguchi E 1982 *J. Phys. Soc. Japan* **51** 3583–91
[6] Shuvaev A T, Helmer B Yu and Lyubeznova T A 1988 *Prib. Tekh. Eksp.* **3** 234–7
[7] Hanske-Petitpiere O, Yacoby Y, Mustre de Leon J, Stern E A and Rehr J J 1991 *Phys. Rev.* B **44** 6700–7
[8] Ravel B, Stern E A, Yacoby Y and Dogan F 1993 *Japan. J. Appl. Phys.* 782–4
[9] Mathuan N, Prouzet E, Husson E and Dexpert H A 1993 *J. Phys.: Condens. Matter* **5** 1261–70
[10] Shuvaeva V A, Antipin M Yu, Lindeman S V, Fesenko O E, Smotrakov V G and Struchkov Yu T 1993 *Ferroelectrics* **141** 307–11